

## THERMAL TRANSMITTANCE OF MULTI-LAYER GLAZING WITH ULTRATHIN INTERNAL PARTITIONS

Agnieszka A. Lechowska<sup>1</sup>, Jacek A. Schnotale<sup>1</sup>

<sup>1</sup>Cracow University of Technology,  
Department of Environmental Engineering,  
ul. Warszawska 24, 31-128 Cracow, Poland

### ABSTRACT

In the paper, the heat transfer through multi-layer glazing has been analyzed. The glazing prototype consists of two standard glass panes (internal and external) and 11 ultra-thin organic glass panes separated by 12 air/argon mixture gaps, all placed in a styrofoam frame. The study of heat transfer through the glazing represented by a two-dimensional CFD model has been conducted using Ansys Fluent CFD software. The numerical simulation results have been compared to analytical calculation data based on EN 673 procedure as well as measurements in the calorimetric hot box instruments in accordance with EN ISO 12567-1 standard.

### INTRODUCTION

In recent times, there has been an increased focus on lowering the energy demands in buildings (Appelfeld et al., 2011, Directives 2010/31/EU and 2012/27/EU) leading to a reduction of transmission heat losses through the building envelopes and the development of buildings that are almost air tight. However windows, to a large degree, still contribute to the total building heat loss with respect both to the cooling and heating demands (Appelfeld et al., 2011). The triple glazed windows are easily available on the market. Their thermal transmittance is about  $U_w = 0,7 \text{ W}/(\text{m}^2\text{K})$ , which is approximately three times more than thermal transmittance of standard walls in buildings.

There has been a lot of effort made to implement windows with low U-values. Different construction solutions have been proposed (Jelle et al., 2012). One of the examples is an "air sandwich" consisting of a number of thin plastic films separated by plastic spacers to arrange air gaps for insulation. The number of air gaps influences the glazing thermal transmittance, which can obtain the value of less than  $0.5 \text{ W}/(\text{m}^2\text{K})$  when 20 plastic layers are applied. The product is still under development. However, there are concerns with the long-term durability of the thin plastic film pack with respect to both polymer degradation by solar radiation and the ability to maintain all plastic films smooth and parallel with no wrinkles.

In the paper a different set up to construct a low U-value multi-layer glazing is proposed. The

developed glazing consists of two standard glass panes (internal and external) and 11 ultra-thin (thickness of 0.4 mm) organic glass panes with 13 mm spacers that arrange 12 argon/air (90%/10% mixture) gas gaps. The number of gas gaps was selected based on calculation with a target value of heat transmittance set to  $0.3 \text{ W}/(\text{m}^2\text{K})$ . If such a low heat transmittance value was achieved the glazing heat transmittance would be comparable to that of opaque building envelope. The glazing prototype with spacers was mounted in a Styrofoam frame. The Ansys Fluent numerical CFD tool has been applied to simulate the heat transfer through the glazing (Dalal et al., 2009, Vendelboe et al., 2008). The glazing geometry was represented by a two-dimensional CFD model. The numerical simulation results have been compared to analytical calculation data based on EN 673 procedure. The calculation procedure takes into account 1-D heat transmission in the central glazing part. The aim of the calculations was to check if the procedure is sufficient for multi-layer glazing examples. The calorimetric hot box instruments were applied to validate numerical modelling and to determine the thermal transmittance of the analyzed glazing (Appelfeld et al., 2011, Asdrubali et al., 2011, Chen et al., 2012, Elmahdy, 1992, Fang et al. 2006, Rose et al., 2004). The measurements were based on EN ISO 12567-1 standard.

### CFD GLAZING MODEL

The glazing model consists of two 4 mm glass layers (internal and external) with low emissivity coatings on both surfaces of the internal gas gaps. The other 11 organic glass layers have a thickness of 0.4 mm. Twelve 13 mm width gas gaps are filled with mixture of argon (90%) and air (10%). The dimensions of the glazing are 623 mm (width), 622 mm (height) and 163 mm (thickness).

A view of the analyzed glazing is given in Figure 1, while the CFD model geometry is presented in Figure 2.

It was assumed that the upper and lower glazing boundary is adiabatic. The spacer influence has not been analyzed.

The CFD calculations were performed with rectangular mesh of about 400,000 cells. The mesh

quality has been checked by two indicators: aspect ratio and skewness. Their values should not exceed 35:1 and 0.95 respectively. In the model the values of 2.1:1 and  $1.3 \cdot 10^{-10}$  were obtained, that indicates the high mesh quality.



Figure 1 The view of the glazing

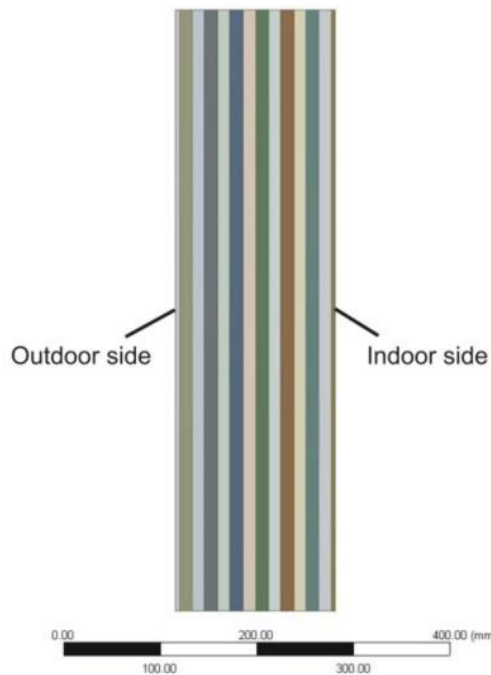


Figure 2 The cross-section of the glazing

Table 1

Material properties applied in the calculations

MATERIAL	$\rho$ kg/m <sup>3</sup>	$\lambda$ W/(mK)	$c_p$ J/(kgK)	$\varepsilon$ –
Glass	2500	1	840	0.837
Glass with low emissivity coating	2500	1	840	0.037
Organic glass	1180	0.19	1260	0.837
Steel	2719	16.3	871	0.2

Thermal properties of the glazing construction materials applied for calculation are listed in Table 1, while gas thermal properties are presented in Table 2.

In Table 1  $\rho$  stands for density,  $\lambda$  – thermal conductivity,  $c_p$  – specific heat,  $\varepsilon$  – emissivity.

Table 2

90% Argon, 10% air mixture thermal properties applied in the calculations

$T$ °C	$\rho$ kg/m <sup>3</sup>	$\lambda$ W/(mK)	$c_p$ J/(kgK)	$\mu$ kg/(ms)
0	1.714	0.0171	567.9	$2.06 \cdot 10^{-5}$
10	1.652	0.0177	567.9	$2.12 \cdot 10^{-5}$
20	1.595	0.0182	567.9	$2.19 \cdot 10^{-5}$

In Table 2  $T$  stands for temperature,  $\mu$  – dynamic viscosity.

Boundary conditions have been set as prescribed for analytical calculations by EN 673 standard. Free external convective heat transfer coefficients of 3.6 W/(m<sup>2</sup>K) and 18.6 W/(m<sup>2</sup>K) were assumed for the internal and external glass surfaces respectively. The indoor and outdoor temperatures were set at 19.9°C and 0.1°C. The same temperatures were set in the calorimetric chamber for tests, as it will be given later, so CFD simulations and laboratory tests were done under the same conditions.

The settings for the finite element CFD model for the convective and radiative heat transfer are listed below:

- solver – stationary,
- viscous model – laminar,
- discretization schemes: gradient - least squares cell based, pressure - body force weighted, momentum and energy - second order upwind,
- radiation model - Discrete Transfer Radiation Model (DTRM).

The total thermal transmittance of the glazing calculated with the use of CFD model was equal to 0.296 W/(m<sup>2</sup>K). It should be mentioned that the value of the transmittance is relatively low, even comparable with thermal transmittance of solid walls in EU buildings.

The calculated temperature distribution and the 90% argon and 10% air mixture velocity vectors in the lower part of the glazing are presented in Figures 3 and 4 respectively.

As it can be seen in Figure 4, the intensity of convective gas movements depends on the gap location. The gas movements are the most intensive in gaps neighbouring external and internal pane. In other gaps the gas velocity is close to zero.

### ANALYTICAL CALCULATIONS

Standard EN 673 gives the procedure of analytical calculations of glazing transmittance for flat and parallel surfaces in the central area of glazing. The standard does not take into account thermal bridges

through the spacer or through the window frame. The procedure has been applied to calculate the glazing transmittance and to compare it with simulation results.

The standardized assumptions for the analytical calculations are given in table 3.

Table 3

Assumptions for analytical calculations

Thermal resistivity of soda lime glass	1 mK/W
Thermal resistivity of organic glass	5.26 mK/W
Temperature difference between bounding glass surfaces	15 K
External heat transfer coefficient for uncoated soda lime glass surfaces	23 W/(m <sup>2</sup> K)
Internal radiative heat transfer coefficient for uncoated soda lime glass surfaces	4.4 W/(m <sup>2</sup> K)
Internal convective heat transfer coefficient for uncoated soda lime glass surfaces	3.6 W/(m <sup>2</sup> K)
Constant in Nusselt number for vertical glazing	0.035
Exponent in Nusselt number for vertical glazing	0.38

The calculation results of the glazing according to EN 673 standard are as follows:

- total thermal conductance of the glazing  $h_t = 0.303 \text{ W}/(\text{m}^2\text{K})$ ,
- thermal transmittance of the glazing  $U = 0.288 \text{ W}/(\text{m}^2\text{K})$ .

The thermal transmittance of the glazing calculated with the EN 673 standard is 3% lower than the value calculated with the Ansys Fluent CFD program. It should be mentioned, that the calculation method described in EN 673 standard takes into account one-dimensional heat flow and the result applies to the central part of the glazing. As it can be seen, the satisfactory agreement between simulations and analytical results has been achieved. To assess calculations accuracy, the experimental validation has been performed using the calorimetric hot box test stand.

## EXPERIMENT

All investigations were performed at Cracow University of Technology. The calorimetric hot box (CHB) was used with the test method in compliance with EN ISO 12567-1 standard. The CHB system consists of a metering box, simulating the indoor environmental condition (warm side), and a climate box, simulating the outdoor environmental condition (cold side).

The metering box is surrounded by a guarding box in order to minimize the heat flow rate through the metering box walls. The test specimen, glazing, is mounted into the opening of a surround panel.

The tested glazing and surround panel are placed between the metering box and the climate box. The steady state heat flow rate through the glazing due to the constant indoor and outdoor temperature difference is measured in order to calculate the glazing thermal transmittance. Figure 5 shows the schematic cross-section of the CHB system in thermal transmittance measurement mode (Chen et al., 2012, EN ISO 12567-1). The view of the CHB system is presented in Figure 6.

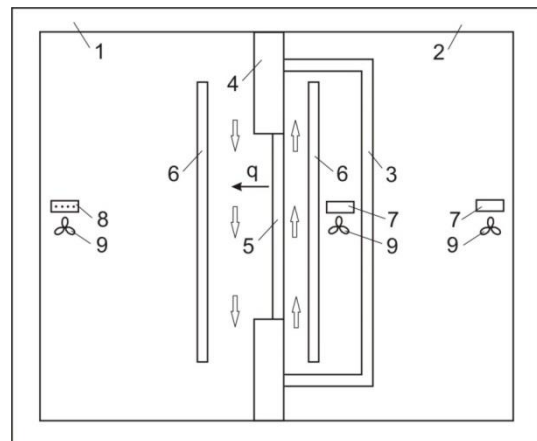


Figure 5 CHB system scheme: 1 – climate box (outdoor side), 2 – guarding box (indoor side), 3 – metering box, 4 – surround panel, 5 – tested specimen, 6 – isothermal baffle, 7 – heater, 8 – cooling element, 9 – fan



Figure 6 General view of calorimetric hot box (CHB) system

The glazing thermal transmittance measurements are divided into two stages. Firstly, the two calibration panels with accurately known thermal properties are tested. The glazing is tested in the second stage of the measurements.

Both calibration panels (with total thickness of 27 mm and 68 mm) were built with the core material of polystyrene and two external layers of 4 mm thick float glass. With known thermal resistances of

calibration panels and surround panel, surface convective and radiative heat transfer coefficients on both sides of the panels are determined. Three measurements of both calibrations panels were taken during the calibration procedure. The fan settings were the same, but there were different air temperatures on cold and hot sides. The measurement results for calibration panels can be seen in Table 4.

Table 4  
Calibration panel measurement results

CALIBR. PANEL 1 (THICKNESS OF 27 mm)				
		Meas. 1	Meas. 2	Meas. 3
$\theta_{ce}$	°C	7.34	0.31	-6.80
$\theta_{se,b}$	°C	7.56	0.56	-6.52
$\theta_{se,cal}$	°C	8.05	1.34	-5.50
$\theta_{se,p}$	°C	7.97	1.18	-5.76
$\theta_{se,sur}$	°C	7.74	0.89	-6.07
$\theta_{ci}$	°C	19.92	19.87	19.87
$\theta_{si,b}$	°C	19.78	19.65	19.57
$\theta_{si,cal}$	°C	18.87	18.27	17.80
$\theta_{si,p}$	°C	18.84	18.36	18.12
$\theta_{si,sur}$	°C	19.80	19.57	19.41
$\Phi_{in}$	W	10.68	15.71	20.70
$v_i$	m/s	0.1	0.1	0.1
$v_e$	m/s	1.7	1.7	1.7
CALIBR. PANEL 2 (THICKNESS OF 68 mm)				
		Meas. 1	Meas. 2	Meas. 3
$\theta_{ce}$	°C	7.43	0.34	-6.78
$\theta_{se,b}$	°C	7.73	0.64	-6.39
$\theta_{se,cal}$	°C	8.69	2.22	-4.34
$\theta_{se,p}$	°C	8.11	1.29	-5.60
$\theta_{se,sur}$	°C	7.80	0.83	-6.05
$\theta_{ci}$	°C	19.81	19.56	19.39
$\theta_{si,b}$	°C	19.50	19.07	18.75
$\theta_{si,cal}$	°C	17.45	15.98	14.66
$\theta_{si,p}$	°C	18.13	17.10	16.24
$\theta_{si,sur}$	°C	19.71	19.29	18.97
$\Phi_{in}$	W	19.70	30.53	41.27
$v_i$	m/s	0.1	0.1	0.1
$v_e$	m/s	1.7	1.7	1.7

In Table 4  $\theta_e$  stands for cold side temperatures and  $\theta_i$  for warm side temperatures of: c – mean air; s,b – baffle surface; s, cal – calibration panel surface; s,p – surround panel reveal surface; s,sur – surround panel surface;  $\Phi_{in}$  – input power to the metering box;  $v_e$  - air velocity on cold side, upwards;  $v_i$  - air velocity on warm side, downwards.

A PID-controller based upon the measured temperature difference across the metering box walls controlled the environment in the guarded box. The cold side temperature is kept with 0.5 % discrepancy of the overall temperature difference in a steady state condition. It was assumed that the stability was attained if within two hours, the measurement results were stable with fluctuations of  $\pm 0.05$  % in the

measured values. Measurements were performed with an accuracy that meets the demands specified in the EN ISO 8990 standard (Rose et al., 2004).

The calibration panel mounted into the surround panel can be seen in Figure 7.



Figure 7 One of calibration panels mounted into the surround panel – warm side view

The results from the calibration measurements can be seen in Figures 8 ÷ 10.

The following regression curves have been calculated with the least-squares method:

$$R_{sur} = 7.9201 - 0.207 \theta_{me,sur} \quad (1)$$

$$F_{c,i} = 0.3074 + 0.0041 q \quad (2)$$

$$F_{c,e} = 0.5931 + 0.0053 q \quad (3)$$

$$R_{s,t} = 0.33 q^{-0.148} \quad (4)$$

with coefficients of determination  $R^2$  equal to values: 0.982; 0.920; 0.887 and 0.942 respectively.

With known convective and radiative fractions of surface resistances, the second stage of the measurements can be started. It is assumed that the emissivity of the calibration panel is similar to the emissivity of the glazing and surface resistances of the calibration panels are similar to the resistances calculated for calibration panels. The glazing measurements are taken with the same fan settings as for calibration panels.

The cold side temperature was kept at a 0.1°C while the metering box was kept at an environmental temperature of 19.9°C using the same kind of PID-controller as the guarded box. The surface resistance on the cold side was established by

controlling the air speed upward along the specimen using a set of regulated ventilators - a similar arrangement as on the warm side of the specimen in the metering box (although the air direction was downward).

Measurement results of glazing prototype are listed in Table 5.

Table 5  
Glazing measurement results

GLAZING (THICKNESS OF 163 mm)		
$\theta_{ce}$	°C	0.11
$\theta_{se,b}$	°C	0.50
$\theta_{se,p}$	°C	1.15
$\theta_{se,sur}$	°C	0.88
$\theta_{ci}$	°C	19.92
$\theta_{si,b}$	°C	19.78
$\theta_{si,sur}$	°C	19.52
$\Phi_{in}$	W	13.81
$v_i$	m/s	0.1
$v_e$	m/s	1.7

The calculation results of the glazing according to the EN ISO 12567-1 standard are as follows:

- heat flow density through the specimen  $q_{sp} = 6.075 \text{ W/m}^2$ ,
- convective fraction - warm side  $F_{ci} = 0.332$ ,
- convective fraction - cold side  $F_{ce} = 0.625$ ,
- total surface resistance  $R_{s,t} = 0.253 \text{ m}^2\text{K/W}$ ,
- radiant temperature - warm side  $\theta_{ri} = 19.78^\circ\text{C}$ ,
- radiant temperature - cold side  $\theta_{re} = 0.50^\circ\text{C}$ ,
- environmental temperature on the warm side  $\theta_{ni} = 19.83^\circ\text{C}$ ,
- environmental temperature on the cold side  $\theta_{ne} = 0.26^\circ\text{C}$ ,
- environmental temperature difference  $\Delta\theta_n = 19.57 \text{ K}$ ,
- thermal transmittance of the glazing (measured)  $U = 0.310 \text{ W}/(\text{m}^2\text{K})$ ,
- total surface resistance (standardized)  $R_{(s,t)st} = 0.17 \text{ m}^2\text{K/W}$ ,
- thermal transmittance of the glazing (standardized)  $U_{st} = 0.319 \text{ W}/(\text{m}^2\text{K})$ .

A total surface resistance of  $0.253 \text{ m}^2\text{K/W}$  was calculated according to measured air velocities and adjacent air temperatures on the warm and cold side. With known total surface resistance, the U value of the glazing calculated according to the measurement results was equal to  $0.310 \text{ W}/(\text{m}^2\text{K})$ . The measured total surface resistance is then replaced by  $0.04 \text{ m}^2\text{K/W}$  on the cold side and  $0.13 \text{ m}^2\text{K/W}$  on the warm side in thermal transmittance calculation procedure. That values with measured glazing resistance let achieve the standardized U value finally equal to  $0.319 \text{ W}/(\text{m}^2\text{K})$ .

With the CHB system, the heat flow through the specimen can be obtained with certain accuracy. The

accuracy in each separate measurement not only depends upon the complexity of the construction being measured, but also on heat exchange with the surroundings, errors of temperature readings, dimensions measurements, input power readings etc. The measurement error is not constant from specimen to specimen.

To determine the uncertainty of the calculated heat transfer coefficient, the uncertainty in each performed measurement was estimated and then combined to give a single value according to the law of propagation based on the root square formula (Appelfeld et al., 2011, Asdrubali et al. 2011, Chen et al., 2012, Elmahdy, 1992, EN ISO 12567-1). The thermal transmittance  $U$  is a function of  $n$  independent variables  $x_k$ , which are known with an uncertainty  $\Delta x_k$ .

The global uncertainty of the thermal transmittance  $\Delta U$  can be written as follows (Asdrubali et al., 2011):

$$\Delta U = \sqrt{\sum_{k=1}^n \left[ \frac{\partial U(x_k)}{\partial x_k} \right]^2} \Delta x_k^2 \quad (5)$$

The glazing thermal transmittance uncertainty depends on the following values of parameters and their uncertainties:

$$\Delta U = \Delta U (H_{sp}, w_{sp}, d_{sp}, H_{sur}, w_{sur}, d_{sur}, \theta_{ci}, \theta_{ce}, \theta_{si,b}, \theta_{se,b}, \theta_{si,sur}, \theta_{se,sur}, \theta_{se,p}, \Phi_{in}) \quad (6)$$

where:

- $U$  - overall heat transfer coefficient,  $\text{W}/(\text{m}^2\text{K})$ ,
- $\theta_{ci}$  - air temperature on hot side, °C,
- $\theta_{ce}$  - air temperature on cold side, °C,
- $\theta_{si,b}$  - baffle surface temperature on hot side, °C,
- $\theta_{se,b}$  - baffle surface temperature on cold side, °C,
- $\theta_{si,sur}$  - surround panel surface temperature on hot side, °C,
- $\theta_{se,sur}$  - surround panel surface temperature on cold side, °C,
- $\theta_{se,p}$  - reveal surface temperature on cold side, °C,
- $d_{sp}$  - specimen thickness, m,
- $d_{sur}$  - surround panel thickness, m,
- $H_{sp}$  - specimen height, m,
- $H_{sur}$  - surround panel height, m,
- $w_{sp}$  - specimen width, m,
- $w_{sur}$  - surround panel width, m,
- $\Phi_{in}$  - input power in hot box, W.

The  $U$ -value uncertainty is connected with the measurement errors of dimensions, temperatures and input power in the hot box, equal to  $0.001 \text{ m}$ ,  $0.1 \text{ K}$  or  $0.01 \text{ K}$  and  $0.52 \text{ W}$  respectively.

The calculated value of the glazing thermal transmittance measurement uncertainty is equal to  $0.070 \text{ W}/(\text{m}^2\text{K})$ , this means a measurement error of about 20%. The reason of such high measurement error is in low probe dimensions and low hot box input power.

## CONCLUSIONS

The *U*-value calculation and measurement results of multi-layer glazing with ultrathin internal glass partitions have been presented. The calorimetric hot box method has been applied for measurements as prescribed in the EN ISO 12567-1 standard.

The measurement results were compared to CFD simulation results as well as analytical calculation results according to EN 673. The result comparison is presented in Table 6.

Table 6

*Measured and calculated results of thermal transmittance (U-value) of multi-layer glazing*

Calculated <i>U</i> -value of glazing – CFD numerical simulation	0.30 (0.296) W/(m <sup>2</sup> K)
Analytically calculated <i>U</i> -value of glazing – calculation according to EN 673	0.29 (0.288) W/(m <sup>2</sup> K)
Measured by a calorimetric hot box CHB system <i>U</i> -value of glazing – measurement results according to EN ISO 12567-1	0.32 (0.319) W/(m <sup>2</sup> K)

It should be mentioned that the calculations according to EN 673 take into account 1-D heat transmission in the central glazing part resulting by the lowest *U*-value obtained by three reported methods. The CFD simulations performed in 2-D model assumed no heat losses through the spacer into the Styrofoam frame and surround panel but take into account the edge of the pane characteristic and give *U*-value slightly higher (difference is 0.01 W/(m<sup>2</sup>K)) than analytical calculation. The measured *U*-value that takes into account all aspects of heat transmittance is the highest of the three reported *U*-values. Nevertheless a satisfactory agreement has been achieved for all three methods with maximum discrepancy of 10% between analytical calculations and measurements and discrepancy of 7% between simulations and measurements.

Proposed multi-layer glazing could be applied in office or residential buildings, as translucent building envelope substituting solid walls that would improve natural lighting without compromising building's low energy requirements. In such cases comparatively high glazing thickness could be acceptable.

## ACKNOWLEDGEMENT

The authors would like to thank Vis Inventis Company for preparing the prototype of multi-layer glazing.

## REFERENCES

Appelfeld D., Svendsen S. 2011. Experimental analysis of energy performance of a ventilated window for heat recovery under controlled conditions, Elsevier, Energy and Buildings, 43, pp. 3200-3207.

- Asdrubali F., Baldinelli G. 2011. Thermal transmittance measurements with the hot box method: calibration, experimental procedures and uncertainty analyses of three different approaches, Energy and Buildings, 43, pp. 1618-1626.
- Chen F., Wittkopf S. K. 2012. Summer condition thermal transmittance measurement of fenestration systems using calorimetric hot box, Elsevier, Energy and Buildings, 53, pp. 47-56.
- Dalal R., Naylor D., Roeleveld D. 2009. A CFD study on convection in a double glazed window with an enclosed pleated blind, Elsevier, Energy and Buildings, 41, pp. 1256-1262.
- Elmahdy A. H. 1992. Heat transmission and R-value of fenestration systems using IRC hot box - procedure and uncertainty analysis, Transactions of ASHRAE, 98, 2.
- Fang Y., Eames P. C., Norton B, Hyde T. J. 2006. Experimental validation of a numerical model for heat transfer in vacuum glazing, Solar Energy, 80, 5, pp. 564-577.
- Jelle B. P, Hynd A., Gustavsen A., Arasteh D., Goudey H., Hart R. 2012. Fenestration of today and tomorrow: A state-of-the-art review and future research opportunities, Solar Energy Materials & Solar Cells, 96, pp. 1-28
- Rose J., Svendsen S. 2004. Validating numerical calculations against guarded hot box measurements, Nordic Journal of Building Physics, 4, pp. 9.
- Vendelboe M. V., Svendsen S., Nielsen T. R. 2008. CFD modelling of 2-D heat transfer in a window construction including glazing and frame, Proceedings of the 8<sup>th</sup> Symposium on Building Physics in the Nordic Countries, Copenhagen.
- Directive 2010/31/EU of the European Parliament and of the Council of 19 May 2010 on the energy performance of buildings, 2010/31/UE.
- Directive 2012/27/EU of the European Parliament and the Council of 25 October 2012 on energy efficiency, 2012/27/UE.
- EN ISO 12567-1. 2010. Thermal performance of windows and doors - Determination of thermal transmittance by the hot-box method - Part 1: Complete windows and doors.
- EN 673. 2011. Glass in building – Determination of thermal transmittance (*U* value) – Calculation method.
- EN ISO 8990. 1998. Thermal insulation- Determination of steady-state thermal transmission – Calibrated and guarded hot box

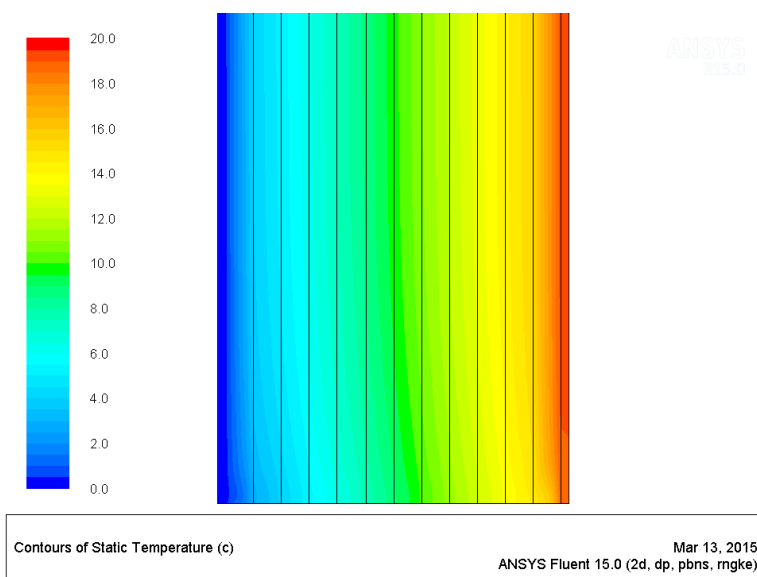


Figure 3 Contours of temperature in the lower part of the glazing

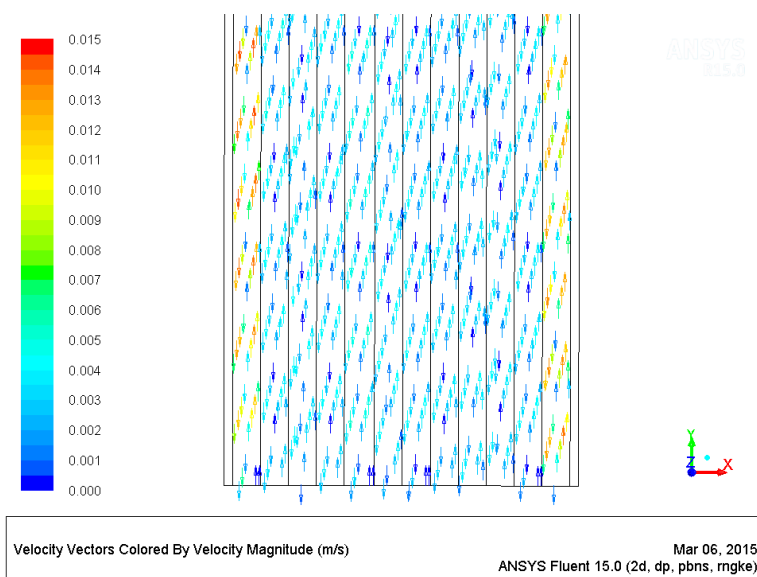


Figure 4 Vectors of gas velocity in the lower part of the glazing

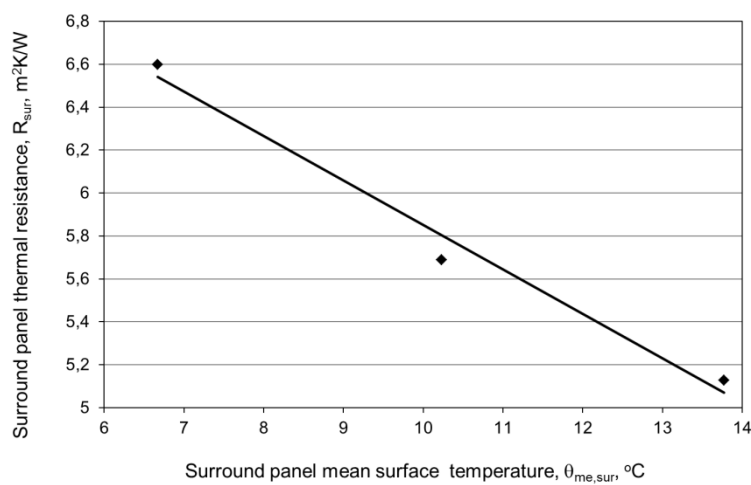


Figure 8 Thermal resistance of the surround panel in terms of the surround panel surface temperature

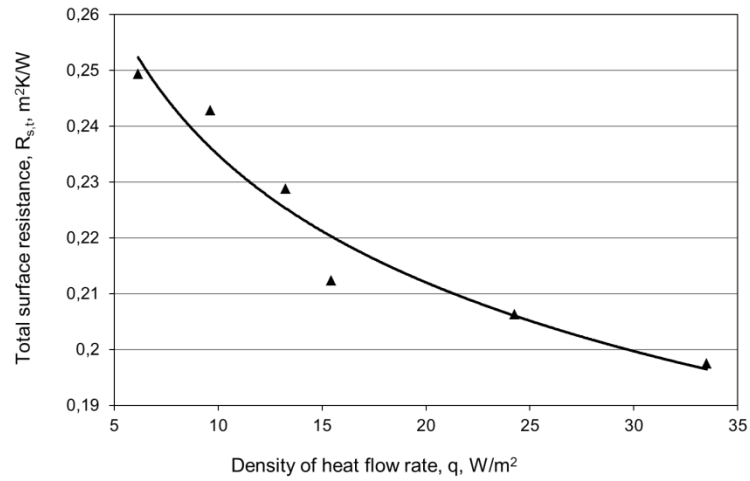


Figure 9 Total surface resistance in terms of density of heat flow rate through the calibration panels

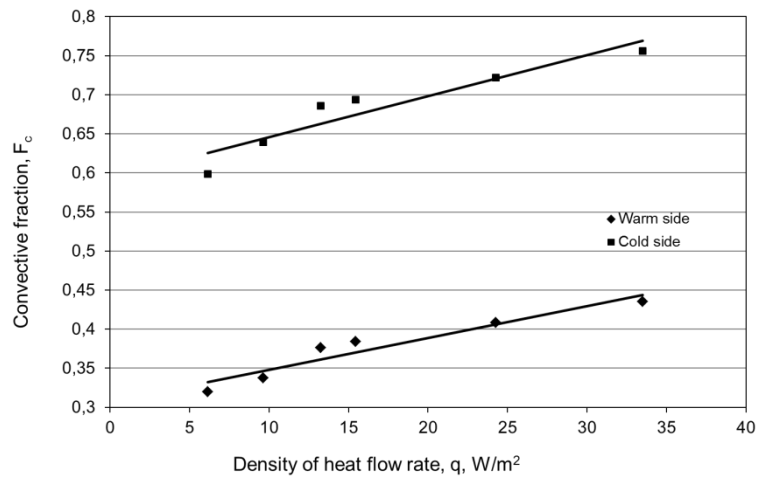


Figure 10 Convective fraction in terms of density of heat flow rate through the calibration panels